 © ASM International

Modeling of the Flow Distribution in an Oil Quench Tank

D.R. Garwood, J.D. Lucas, R.A. Wallis, and J. Ward

This article reports the results of an investigation of the fluid flow in an agitated quench tank used during heat treatment of superalloy forgings. The flow patterns in a scale model of the system were visualized using a laser light sheet and quantitative velocity measurements were undertaken using laser Doppler anemometry (LDA). The experimental data are compared with numerical predictions obtained by means of a computational fluid dynamics (CFD) computer code. Conclusions are drawn as to the suitability of the CFD code for predicting flows in a complex system of this type.

1. Introduction

THE aircraft engine industry is currently attempting to reduce both the development costs associated with new gas turbine engines as well as the lead time between design and production. Consequently, the ability to predict and guarantee the mechanical properties of individual components prior to manufacture has assumed increased importance.

The properties of many superalloy forgings depend, in part, on the cooling rate of the alloy from its solutioning temperature; generally, faster cooling results in higher strength. These alloys are thus typically cooled during heat treatment by quenching in oil or water. Figure 1 (solid lines) shows the experimentally derived relationship between cooling rate and yield strength (at room temperature and at 650 °C) for a nickel-base superalloy material.[1] This information, together with the knowledge of how heat is transferred during quenching, allows mathematical models to be used to predict the cooling rates and hence the properties in a component. Experiments carried out with an instrumented disc, coupled with inverse conduction data analysis, can provide the heat transfer coefficients needed by the models.[2] The application of the above techniques may be seen from the example given in Fig. 1. A finite-element computer code was used to predict the cooling rates in an oil quenched disc. At selected points in the disc, the predicted cooling rate (230 to 300 °C/min) was compared with the yield strength obtained from cut up tests from several forgings. The data points in the figure thus represent the actual property obtained at the predicted cooling rate. It may be seen that these data fall within, or close to, the laboratory-generated property bands (solid lines). A similar analysis was carried out assuming that the disc was forced air cooled. Significantly slower cooling rates were calculated (90 to 135 °C/min), but again the correlation between the observed and the predicted properties is good.

Problems can arise, however, during cooling of disc forgings because the horizontal orientation of the components together with the presence of the support structure in the tank can inhibit the dispersion of vapor and hot fluid formed due to boiling of the quenchant on the lower face of the disc. This can lead to "vapor blanketing" and hence a reduced heat transfer coefficient on this surface.[1,2] This phenomenon, which is generally unpredictable and often inconsistent in practice, affects the ability to accurately predict the properties in a component. In addition, the uneven cooling produced can lead to distortion of the part. The problem can be reduced by designing quench tanks to produce an adequate flow in the quenching region. The present study is thus concerned with experimental and numerical modeling of the fluid flow in a large oil quenching facility. The installation is illustrated in Fig. 2, which shows how a tray of discs is lowered into the tank by means of an elevator structure. The oil is circulated within the tank by means of four impellers mounted near the corners.

A commercially available computational fluid dynamics (CFD) computer code was employed to predict the flow field

D.R. Garwood, J.D. Lucas, and **J. Ward,** The University of Glamorgan, Pontypridd, Wales, United Kingdom, and **R.A. Wallis,** Cooper Industries, Cameron Forged Products Division, Houston, Texas.

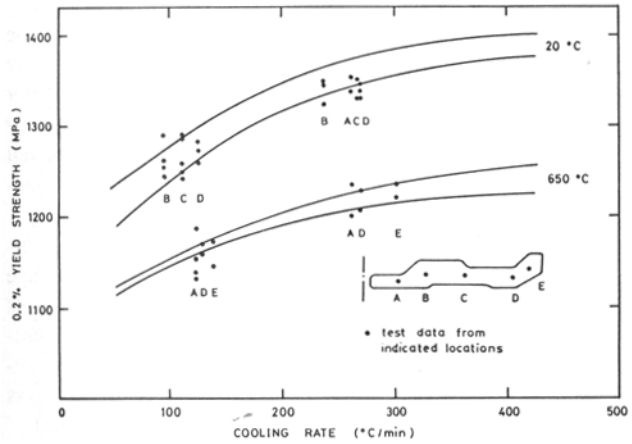

Fig. 1 Yield strength as a function of cooling rate with test data for forced air cooled and oil quenched parts.

Nomenclature

d_f	Characteristic dimension for the full-scale system, m
d_m	Characteristic dimension for the model, m
D_f	Impeller diameter for the full-scale system, m
D_m	Impeller diameter for the model, m
H	Water level in the model tank, m
L	Width of the model tank, m
U_f	Linear velocity in the full-scale system, m/s
U_m	Linear velocity in the model, m/s
x	Distance measured across the model tank, m
y	Distance measured down from the fluid surface, m
ω_f	Rotational speed of the full-scale impeller, rev/min
ω_m	Rotational speed of the model impeller, rev/min
ν_f	Kinematic viscosity of the oil, m^2/s
ν_m	Kinematic viscosity of water, m^2/s

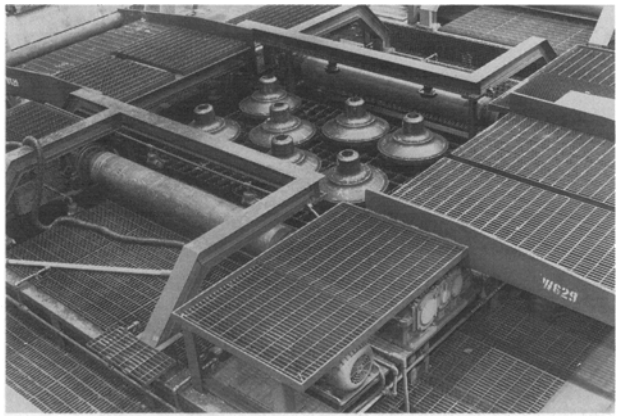

Fig. 2 Oil quench tank showing discs on elevator system.

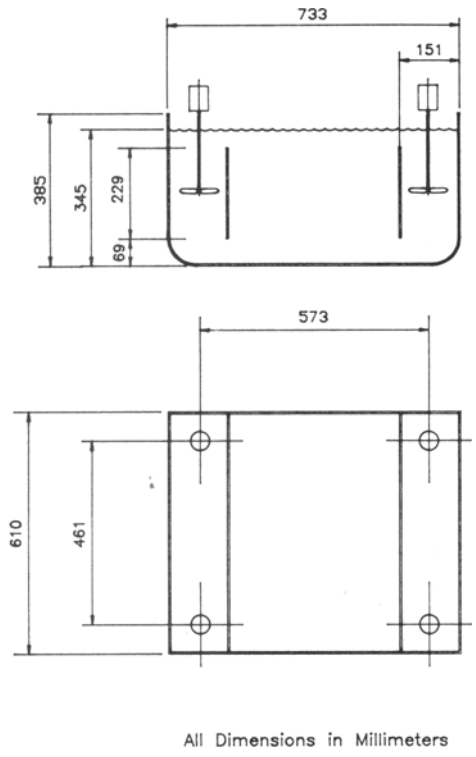

Fig. 3 Details of model tank.

within the quenchant. These predictions are compared with experimental data obtained on a small-scale water model of the system. Tracer techniques were used for qualitative flow visualization purposes, and quantitative velocity measurements were obtained using laser Doppler anemometry.

2. Experimental Arrangements

The experimental measurements were undertaken on a one-seventh scale water model of the production installation (Fig. 3). This model was constructed from 12-mm thick acrylic sheet

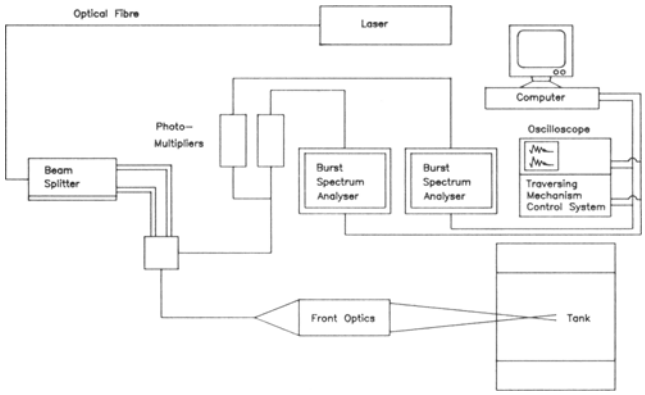

Fig. 4 Schematic of laser Doppler anemometry equipment.

to provide ready access for flow visualization and velocity measurements. A scale model of the elevator system was also incorporated when required. Vertical baffles were positioned across the full width of the tank to assist in guiding the flow into the central quenching region. The four impellers, which were also geometrically scaled, are of a straight blade design with a forward sloping attack angle of 30°. Each impeller was rotated in the same direction by means of individually coupled 12 V DC motors whose speed of rotation was continuously monitored and controlled electronically.

The laser Doppler anemometer that was used for velocity measurements within the model tank was a two-component, two-color, fiber optic system incorporating a Coherent Innova 5-W argon ion laser (see Fig. 4). Horizontal velocities were measured using green light of wavelength 514.5 nm, whereas blue light of wavelength 488 nm was used to yield the vertical velocities. Each laser beam was split and the separate components transmitted along a fiber optic link to the front end optics, which consisted of a 600-mm focal length lens that offered an initial beam separation of 70 mm. The points of intersection of the two beams of each color formed the measurement subvolumes. The lens was mounted on a computer-controlled, three-dimensional traversing mechanism so that the measurement position could be moved automatically within the model tank.

The system was operated in the back-scatter mode, and the signals from the two measurement volumes were processed by Dantec-type 57 N10 burst spectrum analyzers. A minicomputer was used for data acquisition and reduction, and the proprietary software yielded simultaneous mean and rms velocities, as well as turbulence intensity for both the horizontal and vertical components.

The estimated position of the measurement volume was corrected to allow for refraction of the laser beams during passage through the acrylic wall of the model and into the water. This beam distortion also altered the fringe spacing within the measurement volume, and the velocity measurements were corrected to allow for this effect. A small amount of seeding was introduced into the water to enhance the data transfer rate.

Laser Doppler traverses were undertaken directly under the impeller to provide velocity data, in the vertical and two horizontal directions, and these measurements were used as initial

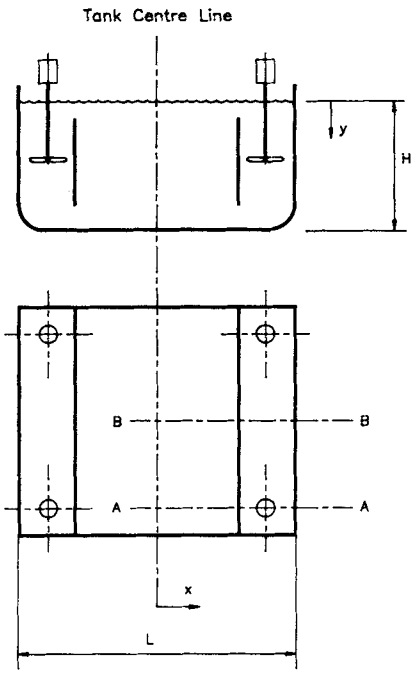

Fig. 5 Positions of LDA traverses for comparison with numerical predictions.

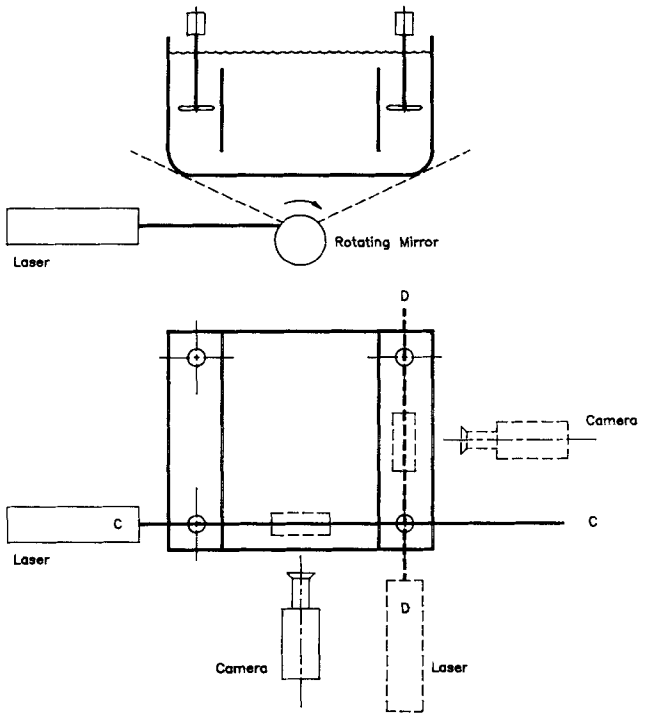

Fig. 6 Flow visualization setup.

input into the computational fluid dynamics model. For comparison with the numerical predictions, velocity measurements were also undertaken in the main section of the tank at various depths on two vertical planes (see Fig. 5).

The flow visualization studies were carried out using a 2-W argon ion laser as the light source. The laser beam was reflected by a prism that was rotated at a speed of 6000 rpm. This arrangement produced a continuous narrow sheet of laser light that could be used to illuminate a plane within the model tank. The optical system was positioned beneath the tank so that a number of vertical planes were illuminated, and the camera and videorecording equipment were positioned at right angles to the illuminated plane (see Fig. 6). The water was seeded with polystyrene spheres of approximately 1 mm diameter to act as tracers.

3. Similarity Criteria

These criteria must be satisfied to ensure that the velocity fields in the water model are representative of those in the full-size oil tank. Geometric similarity was obtained by construction of a scale model as described in the previous section. For totally immersed bodies, dynamic similarity, *i.e.*, similarity of the forces within the fluids, is usually achieved by equating the Reynolds numbers for the model and full-size systems. Thus, for the flows around the components to be similar, this implies that:

$$\frac{U_m}{U_f} = \left(\frac{d_f}{d_m}\right)\left(\frac{\nu_m}{\nu_f}\right) \qquad [1]$$

where the subscripts m and f refer to the model and the full-size installation, respectively, and U is the fluid velocity, ν is the fluid kinematic viscosity, and d is a characteristic dimension for the system. The kinematic viscosity of the oil is 4.5×10^{-5} m^2/s at 43 °C (*i.e.*, a typical operating temperature in the production installation), and this value coupled with the geometric scale factor of one seventh (1/7) yields the following velocity ratio for a water model at a temperature of 20 °C:

$$\frac{U_m}{U_f} = 0.155 \qquad [2]$$

Thus, in a dynamically similar water model, the velocities will be approximately one sixth of those in the actual quench tank.

The rotational speed of the model impellers can be specified from dynamic similarity considerations. This criterion will be satisfied if the model and full-size impellers have the same flow coefficient, and this can be simplified to:

$$\frac{\omega_m}{\omega_f} = \left(\frac{U_m}{U_f}\right)\left(\frac{D_f}{D_m}\right) \qquad [3]$$

where ω is the rotational speed, and D is the impeller diameter. Equations 2 and 3 together with the geometric scale factor yield:

$$\frac{\omega_m}{\omega_f} = 1.09 \qquad [4]$$

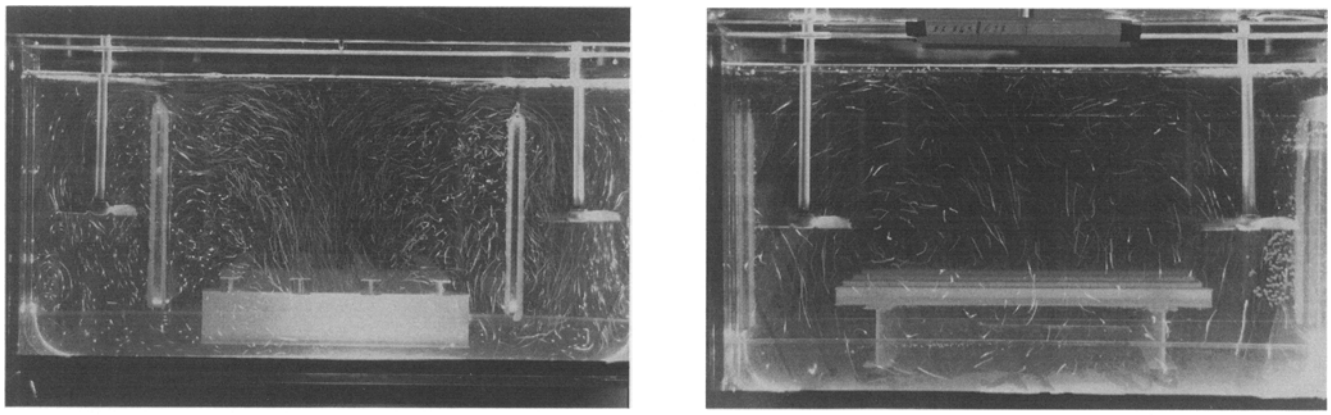

(a) (b)

Fig. 7 (a) Flow visualization photograph, section C-C. (b) Flow visualization photograph, section D-D.

Thus, it was necessary to operate the model impellers with a rotational speed of 245 rpm to achieve dynamic similarity.

4. Computational Model

The flow distributions in both the model and full-size tanks were simulated mathematically using "Fluent," a commercially available computational fluid dynamics package. This computer code uses a numerical finite-difference scheme to solve the Navier-Stokes equations, *i.e.*, the fundamental partial differential equations that govern fluid flow. The finite-difference approximations of these equations are solved at a series of grid points within the fluid, and in the present study, the complicated three-dimensional nature of the flow necessitated the use of the 30,000 points, which were available in the software package. The size of the mesh was varied throughout the tank, with a finer mesh formulated in regions with high-velocity gradients, *e.g.*, near the impellers. A power-law variation was used for interpolation between grid points and for calculation of the derivatives of the flow variables. As mentioned previously, the measured velocity values near the impellers were used as input data to the numerical simulation. Several turbulence models can be accessed in Fluent, and a standard K-ε model was used for this investigation.

5. Results and Discussion

Examples of the flow visualization photographs produced with the laser light sheet are shown in Fig. 7(a) and (b). The light sheet, having a width of approximately 1 mm, provides a two-dimensional view of a section through the tank. Figure 7(a) is taken on a section C-C, and Fig. 7(b) on a section D-D, as shown in Fig. 6.

From Fig. 7(a), it is clear that the flow into the center section of the tank from both impellers is not symmetrical. The front right impeller produces a much stronger flow, both under the baffle and subsequently in the main quench area. The velocities from the left impeller are clearly much weaker at this section. Other features that become apparent from this photograph are the low-velocity areas adjacent to the baffles, in the center region, and near the surface of the liquid itself. The asymmetric nature of the flow can be explained if the direction of the rotation of the impellers is considered with respect to the walls of the tank and the baffle. All impellers are rotating clockwise when viewed from the shaft end, and therefore, the right impeller in Fig. 7(a) is rotating toward the baffle at the front wall. The flow, therefore, is strongly channelled under the baffle as shown. On the left side, the rotation toward the baffle is on the opposite side of the impeller, and the flow is not channeled by the presence of a wall, but is free to diffuse toward the center of the tank. For the flow to be symmetrical, the geometry of the impellers would need to be changed and the direction of rotation reversed.

Figure 7(b), which is taken on a section behind the baffle as described earlier, again shows this asymmetry, which results in a highly three-dimensional flow regime. The recirculating flows in this region are moreover much stronger than in the center of the tank. Thus, the baffles do not appear to achieve their primary purpose of guiding flow into the quench zone.

As mentioned previously, the three-dimensional computational predictions for Fluent were restricted to 30,000 node points, and therefore, the restrictions on grid size made it difficult to model the situation accurately. This was the case when attempts were made to include details of the elevator structure, because a very fine grid would be required near the support. It was, therefore, decided to omit the elevator in the computational model and during the LDA measurements. In this way, comparison could be made between the two sets of data both quantitatively and qualitatively. However, although the elevator is omitted, it is interesting to note that the Fluent predictions (see Fig 8a and b), for the same sections as those in the flow visualization photographs, show the same flow features, (*i.e.*, a very strong recirculation behind the baffles and a nonsymmetrical flow). The three-dimensional nature of the flow is clear

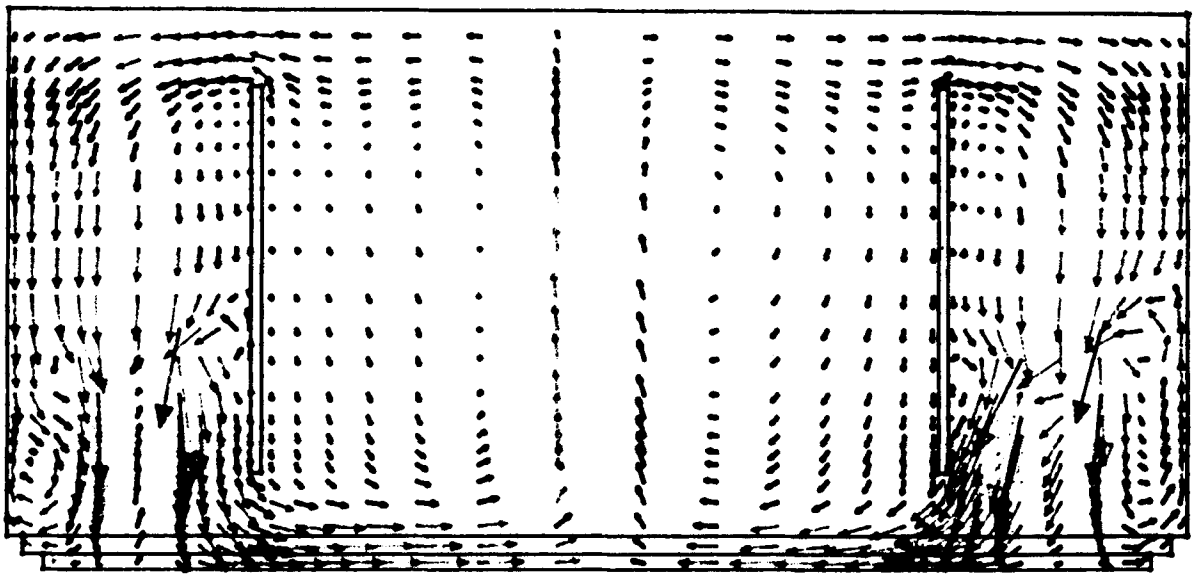

(a)

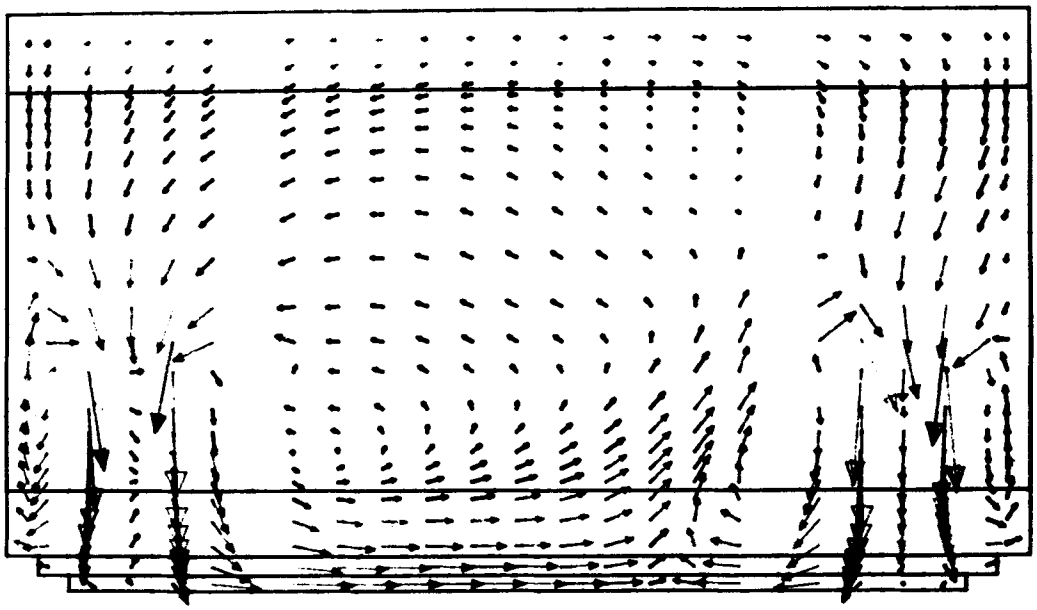

(b)

Fig. 8 (a) Fluent velocity predictions, section C-C. (b) Fluent velocity predictions, section D-D.

from a plan view of the numerical predictions taken at a position below the baffles, near the tank bottom (see Fig. 9).

The laser Doppler anemometer velocity results are compared with the corresponding three-dimensional Fluent predictions in Fig. 10 and 11. The profiles of vertical velocity are presented at vertical stations $y/H = 0.072$, 0.144, 0.44 and 0.56 as measured from the water surface for the two sections shown in Fig. 5. To achieve an accurate half-tank profile at each station, the origin of the velocity measurements was taken as a point 25 mm beyond the tank centerline. The four vertical positions chosen for comparison purposes represent areas near the surface ($y/H = 0.072$ and 0.144) and in the quench region ($y/H = 0.44$ and 0.56).

With reference to Fig. 10 and 11, it is clear that there is closer agreement between the experimental and numerical results at section B-B than at section A-A. For the former section on the centerline of the tank, there is excellent agreement between the measured laser results and the Fluent computational predictions near the water surface, *i.e.*, at $y/H = 0.072$ and 0.144. However, in the quench region at $y/H = 0.44$ and 0.56, the quantitative agreement is not as good, although similarly shaped velocity profiles are predicted by Fluent. For this section at the

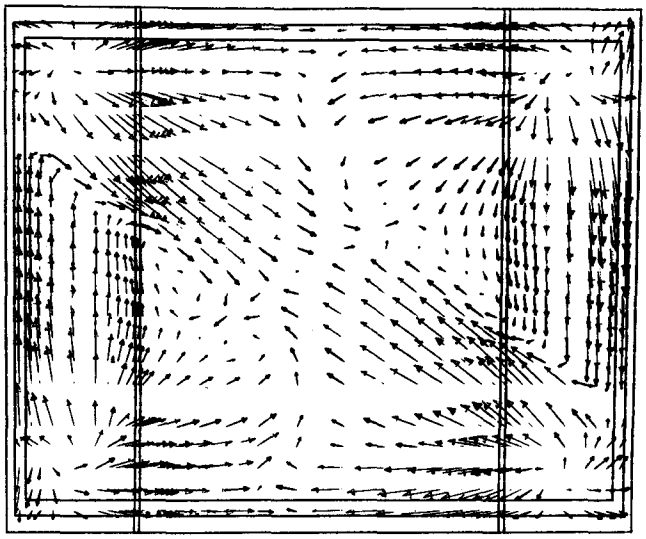

Fig. 9 Fluent velocity prediction showing three-dimensional nature of flow.

center of the tank, all of the numerical profiles show the maximum velocity occurring at a distance approximately 25 mm from the tank centerline, with the magnitude of this maximum vertical velocity increasing with distance from the water surface. The location of the maximum velocity corresponds to a normalized position $x/L = 0.34$, and this again indicates that the flow is not symmetrical.

At the section A-A, along the impeller centerline, agreement is less good. Although generally the profiles of velocity are similar, the quantitative results show a considerable amount of scatter. However, it should be noted that this is a region with high-velocity gradients, high turbulence intensity, and flow reversals. This is particularly true for the area close to the centerline of the tank, which is a region of unstable flow and where significant scatter in the data was obtained. The laser results at $x = 0$ and 25 mm are therefore omitted from Fig. 10.

At a depth $y/H = 0.56$, the recirculation of the flow is clearly visible, with a downward velocity near the baffle region and an upward velocity near the tank center. For the profiles near the water surface ($y/H = 0.072$ and 0.144), the vertical velocities in the baffle area are very small, with an increase toward the tank center. The flow visualization photographs also highlighted the low-velocity areas near the surface in the vicinity of the baffles so that there is good qualitative agreement between experimental and numerical results.

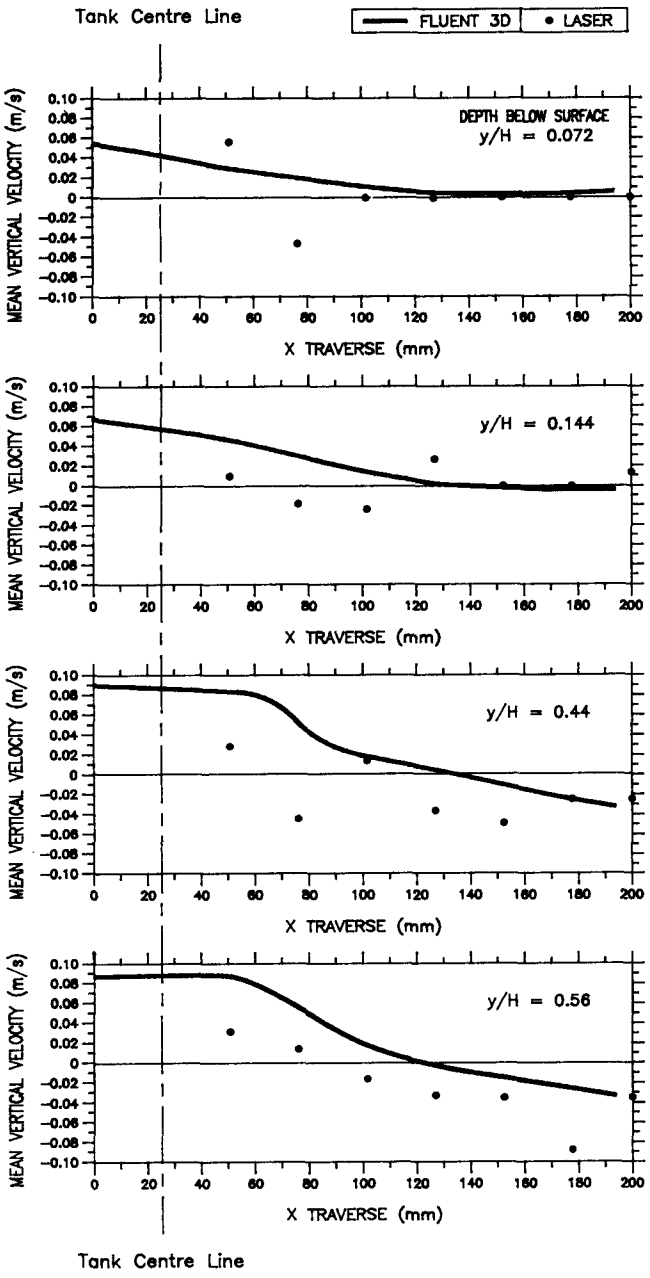

Fig. 10 Profiles of vertical velocity at section A-A.

6. Conclusions

The highly complex flows occurring in an agitated quench tank have been modeled, with the aim that a better understanding of the fluid movement will enable alternative tank designs or modifications to be compared. The computational fluid dynamics computer code was able to predict qualitatively the main flow features in the quenchant. Moreover, the quantitative predictions are in good agreement with the measured velocities in the center of the tank near the water surface. In other parts of the tank, the predictions are less accurate.

Because of the highly three-dimensional nature of the flow and because the limitation of the number of grid points available in the CFD package, it was not possible to model the tank elevator. The presence of this support structure is likely to complicate the flow patterns even further, making the numerical predictions even less accurate. Consequently, because the flow visualization study highlighted the important flow features, this type of qualitative investigation appears to be the most economical method of investigating the effect of alternative tank designs or modifications.

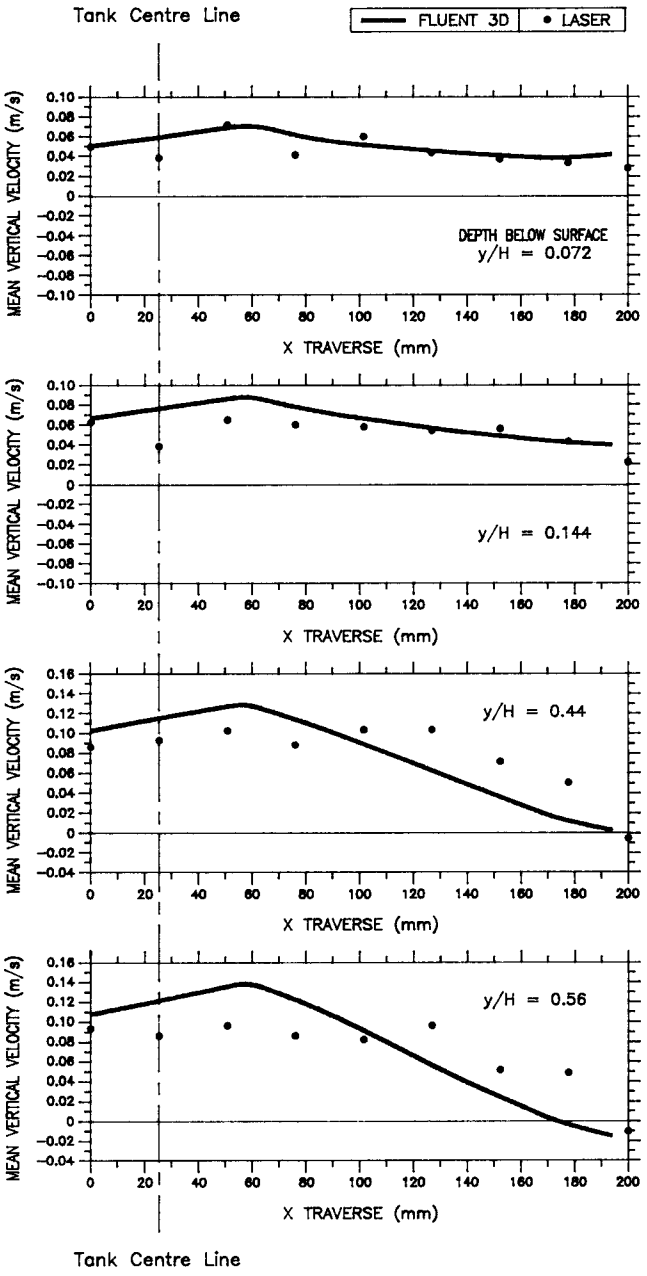

Fig. 11 Profiles of vertical velocity at section B-B.

References

1. R.A. Wallis, P.R. Bhowal, N.M. Bhathena, and E.L. Raymond, Modeling the Heat Treatment of Superalloy Forgings, *JOM*, Vol 41 (No. 2), Feb 1989, p 35-37
2. R.A. Wallis, Using Computer Programs to Calculate Heat Transfer, *Heat Treating*, Vol 21 (No. 12), Dec 1989, p 26, 27, 31